ARTICLES
PUBLISHED ONLINE: 4 APRIL 2016 | DOI: 10.1038/NPHYS3714
nature physics

Laser cooling and control of excitations in superfluid helium

G. I. Harris†, D. L. McAuslan†, E. Sheridan, Y. Sachkou, C. Baker and W. P. Bowen*

Superfluidity is a quantum state of matter that exists macroscopically in helium at low temperatures. The elementary excitations in superfluid helium have been probed with great success using techniques such as neutron and light scattering. However, measurements of phonon excitations have so far been limited to average thermodynamic properties or the driven response far out of thermal equilibrium. Here, we use cavity optomechanics to probe the thermodynamics of phonon excitations in real time. Furthermore, strong light–matter interactions allow both laser cooling and amplification. This represents a new tool to observe and control superfluid excitations that may provide insight into phonon–phonon interactions, quantized vortices and two-dimensional phenomena such as the Berezinskii–Kosterlitz–Thouless transition. The third sound modes studied here also offer a pathway towards quantum optomechanics with thin superfluid films, including the prospect of femtogram masses, high mechanical quality factors, strong phonon–phonon and phonon–vortex interactions, and self-assembly into complex geometries with sub-nanometre feature size.

Elementary excitations, in the form of phonons and rotons, are fundamental to both the macroscopic and microscopic behaviour of superfluid helium-4, including phenomena such as dissipation[1,2], quantum turbulence[3] and phase transitions[4]. Techniques to probe such excitations have been crucial to our understanding of superfluids since the 1960s[5]. For instance, neutron and light scattering[5–7] allow the dynamic structure factor to be determined, which quantifies the dispersion relation, as well as the mean occupancy and correlations. However, such techniques are slow compared to the characteristic dissipation rate of the excitations, constraining them to average thermodynamic properties and prohibiting real-time measurement and control. Whereas the thermodynamic motion of quantized vortices has been tracked in real time as they interact with each other and with phonons (see for example ref. 8), the amplitude of superfluid phonon excitations has until now only been directly observable by coherently driving individual modes far out of thermal equilibrium using an external driving force (see for example refs 1,2,9,10).

In cavity optomechanics, the coupling between optical and mechanical degrees of freedom, and therefore measurement precision, is greatly enhanced by the presence of a high-quality optical cavity. This has enabled the demonstration of a range of quantum behaviours (see for instance[11–16]); measurement precision exceeding fundamental limits set by quantum uncertainty[17–19]; and precision sensors of mass, acceleration and magnetic fields[20–22]. Excitations in superfluids have recently been identified as an attractive mechanical degree-of-freedom[10,23]; introducing unique features such as viscosity that approaches zero at absolute zero, quantized rotational motion and vortices[24], and strong phonon–phonon interactions[5]. In the only previous experiment, a pressure wave in bulk helium acts as a gram-scale resonator[10], with the combination of high mechanical quality factor and mass providing a path towards ultra-precise inertial sensors. However, the comparatively large mass presents significant challenges for the observation or control of thermal excitations, and the manifestation of quantum effects.

Here we propose and use an alternative approach to superfluid optomechanics based on femtogram films of superfluid helium condensed on the surface of a microscale whispering-gallery-mode resonator (Fig. 1a). Superfluid films form naturally on surfaces owing to the combination of ultralow viscosity and attractive van der Waals forces. Excitations in such films, known as third sound[1,2,26,27], manifest as perturbations to the thickness, with the restoring force provided by the van der Waals interaction. The physical structure of the resonator provides a template for the self-assembling film, acting to confine third sound modes at the microscale in two dimensions, with film thickness defining the third dimension. Optomechanical coupling is realized via the optical evanescent field[28], with the film being naturally located in the region of maximum field strength. Compared with previous third sound experiments that use centimetre-scale enclosures and capacitive measurements, this architecture enables a reduction of three orders of magnitude in volume with superfluid mass in the pico- to femtogram range (see Supplementary Information, Section II), combined with greatly enhanced readout sensitivity[1,2,27].

Thin-film superfluid optomechanics

To experimentally realize thin-film superfluid optomechanics, a fibre-coupled microtoroidal resonator is placed in a low-pressure helium-4 gas environment within a helium-3 cryostat (Fig. 1b). At the pressures used, the helium gas transitions directly to the superfluid state at approximately 1 K (see Supplementary Fig. 7), avoiding the normal fluid phase. Van der Waals forces then coat the surface of the sample chamber with a film of superfluid helium. A typical optical resonance lineshape is seen at temperatures above the gas-to-superfluid transition (Fig. 2a (blue)). Below the transition, unstable oscillations appear on the blue-detuned side of resonance (Fig. 2a (orange, green)), characteristic of optomechanical parametric instability where optical dynamical backaction introduces gain that results in a net amplification of mechanical motion[29]. This is observed with as little as 40 nW of

Centre for Engineered Quantum Systems, School of Mathematics and Physics, University of Queensland, Brisbane, Queensland 4072, Australia. †These authors contributed equally to this work. *e-mail: w.bowen@uq.edu.au

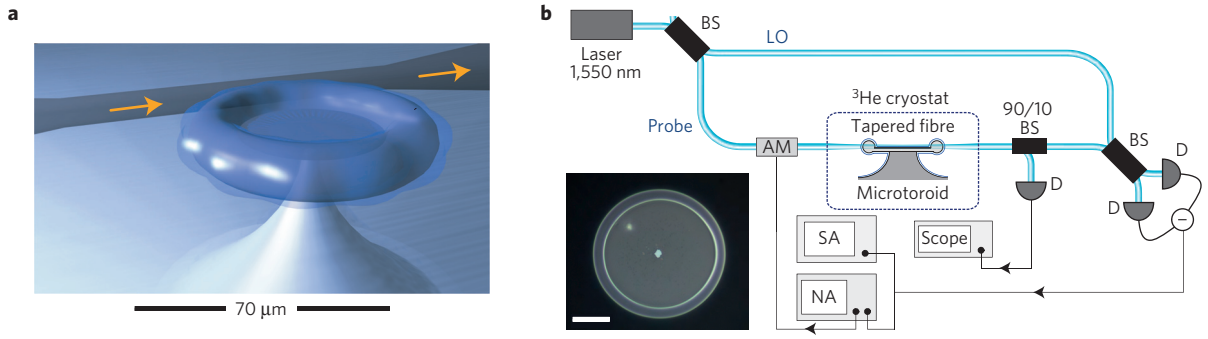

Figure 1 | Optomechanics with superfluid helium films. a, Illustration of third sound waves of a superfluid helium film coating a microtoroid. The third sound oscillations have phase velocity $C_3 = \sqrt{3\alpha_{vdw} d^{-3}}$, where $\alpha_{vdw} = 2.65 \times 10^{21}$ nm^5 s^{-2} is the van der Waals coefficient for silica and d is the thickness of the superfluid film. **b**, Shot-noise limited homodyne detection of superfluid helium optomechanics. A tapered fibre-coupled microtoroid (major diameter = 75 μm, minor diameter = 7 μm), which was fabricated by means of photolithography and CO_2 laser reflow, as described in ref. 25, is mounted inside the sample chamber of a helium-3 cryostat. Helium-4 gas is injected into the sample chamber at a pressure of 69 mtorr (at 2.8 K). AM—amplitude modulator, BS—beamsplitter, D—photodetector, NA/SA—network/spectrum analyser. The 90/10 BS probes the optical transmission through the microtoroid. At the base temperature of the cryostat the superfluid film is roughly 10 nm thick. Inset: optical microscope image of the microtoroid used in the experiment, exhibiting a defect on the central silica disk (bright spot, top left); scale bar, 20 μm.

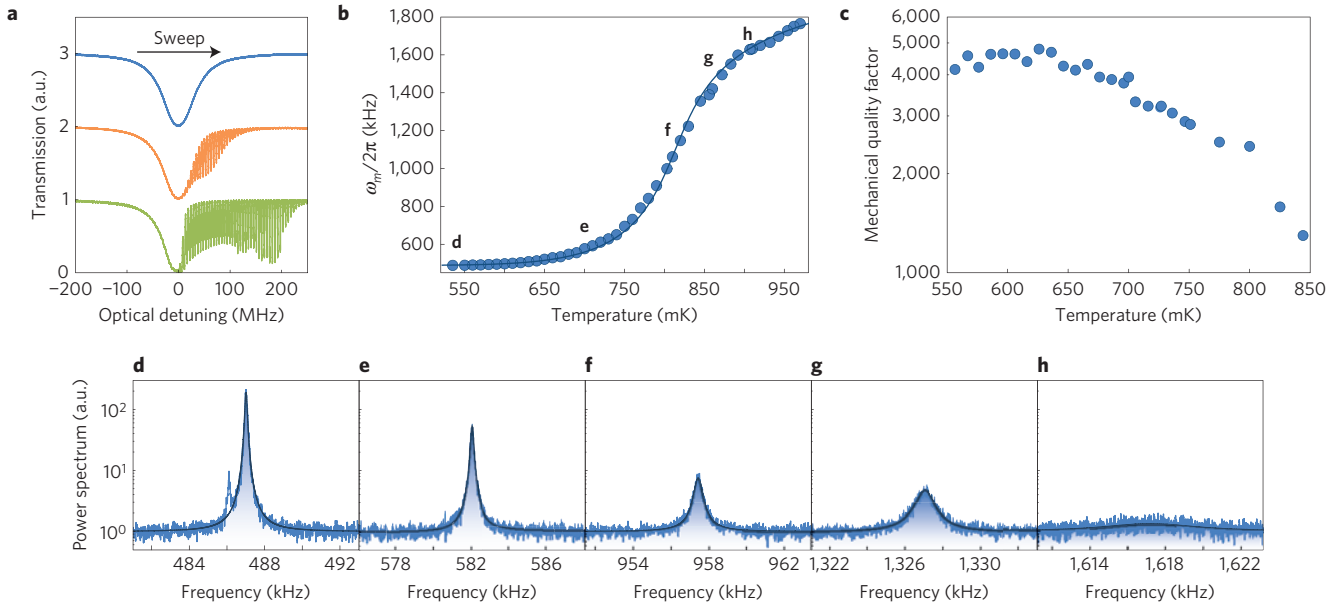

Figure 2 | Superfluid helium mechanics. a, Observation of superfluid oscillations as the cryostat cools to base temperature, while the laser frequency is scanned and optical resonance tracked. Blue, orange and green traces are offset vertically and were respectively taken at 3 K, 1 K and 0.6 K. **b**, Resonance frequency of a particular superfluid mode versus cryostat temperature, with a final frequency of 482 kHz. The resonance frequency was tracked by means of network analysis as the cryostat temperature was varied. The solid line is a theoretical fit obtained by modelling the condensation of the helium gas. **c**, Mechanical quality factor of the superfluid mode versus cryostat temperature, measured by means of spectral analysis of the thermomechanical motion. Note that, above 850 mK, the signal-to-noise ratio was too low to accurately measure the quality factor. **d**–**h**, Mechanical spectra of the superfluid mode at the cryostat temperatures indicated in **b**: 530, 700, 800, 850 and 900 mK (from left to right). These measurements were performed with the laser coupled to a microtoroid optical mode at $\lambda = 1{,}555.1$ nm with optical decay rate $\kappa/2\pi = 22.3$ MHz. We note that superfluid oscillations have been proposed previously as a possible source of periodic features observed in the driven response of a cryogenic microtoroidal resonator[30], although only limited investigations were performed.

optical power, over one hundred times lower than would be expected from a microtoroid mechanical mode[29].

To characterize the mechanical response of the superfluid film we lock the laser to an optical resonance of the microtoroid. Heating due to optical absorption at the periphery of the microtoroid generates a photoconvective superfluid flow through the superfluid fountain effect[31]. Owing to their spatial overlap with this flow field, we find that the third sound modes can be coherently driven by an optical amplitude modulation (see Supplementary Information VI). This driven motion is encoded on the phase of the optical field, which is monitored by means of homodyne detection. Sweeping the modulation frequency, a dense spectrum of mechanical modes is observed (see Supplementary Information IV), ranging in frequencies from 10 kHz to 5 MHz, consistent with third sound modes confined to length scales on the order of the microtoroid dimensions. The modes tend to exist in near-degenerate pairs, separated in frequency by several hundred hertz. We attribute this splitting to a breaking of cylindrical symmetry due to scattering by a defect on the microtoroid surface (see inset, Fig. 1b). Owing to the dense mode spectrum and uncertainties

in experimental parameters, such as microtoroid geometry, film thickness and boundary conditions, it was not possible to resolve the exact mode shapes. However, finite element modelling qualitatively reproduces the observed mechanical spectrum (see Supplementary Information II). As the cryostat cools, the frequency of the superfluid modes is observed to decrease (Fig. 2b). This occurs owing to increased condensation of helium into the superfluid film, with thickening of the film resulting in a weaker van der Waals mediated restoring force. The low-temperature plateau in frequency, evident in Fig. 2b, occurs when the majority of gaseous helium in the sample chamber has been condensed into the superfluid phase, resulting in a mechanical frequency that can be precisely tuned by injecting or evacuating helium gas.

Observation and tracking of thermally driven motion

When coupled to a thermal bath at temperature T, the root-mean-square motional amplitude of an oscillator is given by equipartition to be $\delta x = \sqrt{k_B T/k}$, where k is the spring constant of the oscillator and k_B is the Boltzmann constant. The motion decorrelates over a characteristic timescale of $1/\Gamma_m$, where Γ_m is the oscillator decay rate. Only if measurement precision better than δx is achieved within this timescale, is it possible to track the thermally driven trajectory of the oscillator in phase space. This allows thermodynamic fluctuations to be studied and controlled in real time, and the fundamental thermomechanical noise floor of force and inertial sensing to be reached. As discussed in Supplementary Information VII, this ability to make a real-time measurement of the amplitude of thermodynamic fluctuations corresponds to achieving a signal-to-noise ratio (SNR) greater than one in the power spectral density of the measurement. Although many techniques have been developed to probe the thermal properties of phonon excitations in superfluid helium, it has proved difficult to achieve this regime. For instance, the light scattering measurements in ref. 7 averaged photocounts for around 30 min to retrieve the thermal motion spectrum of first sound waves, whereas the recent work of De Lorenzo and Schwab[10] remains six orders of magnitude away from resolving the thermal motion.

The reduced mode volume and strong evanescent optomechanical coupling achieved in our architecture combine to greatly enhance the capacity to resolve thermodynamic fluctuations. To test whether real-time measurements are possible, we perform homodyne-based phase measurement. Spectral analysis on a high-quality third sound mode at 482 kHz reveals a thermomechanical noise peak characteristic of mechanical oscillations (see Fig. 2d–h) with a SNR of 21 dB, substantially exceeding unity, and therefore providing the ability to measure the superfluid motion in real time. It was observed that the mechanical quality factor increases substantially with decreasing temperature (Fig. 2c), consistent with previous observations attributed to phonon–vortex interactions[1,24], with the dissipation rate reaching a minimum of $\Gamma_m/2\pi = 106$ Hz at 530 mK.

To demonstrate real-time measurement, we recorded the homodyne output photocurrent for a period of 5 s. Mixing this signal down with a sine wave and filtering with a single-sided exponential with decay constant equal to Γ_m (see Fig. 3b), yielded a (unnormalized) best estimate of the X-quadrature amplitude of the superfluid mode as a function of time (orange trace in Fig. 3a). For comparison, a short-time estimate (blue trace in Fig. 3a) was obtained by truncating the exponential filter (Fig. 3c) to a finite measurement duration τ. When the measurement time τ is shorter than the mechanical dissipation time ($1/\Gamma_m$), the variance V of the difference between the two estimates is dominated by the uncertainty in the short-time estimate. The variance is shown as a function of τ in Fig. 3d, normalized to the thermal variance V_T. As can be seen, the superfluid motion can be tracked with precision superior to the thermal variance on timescales significantly shorter than the mechanical decay time. The quadrature is localized to half

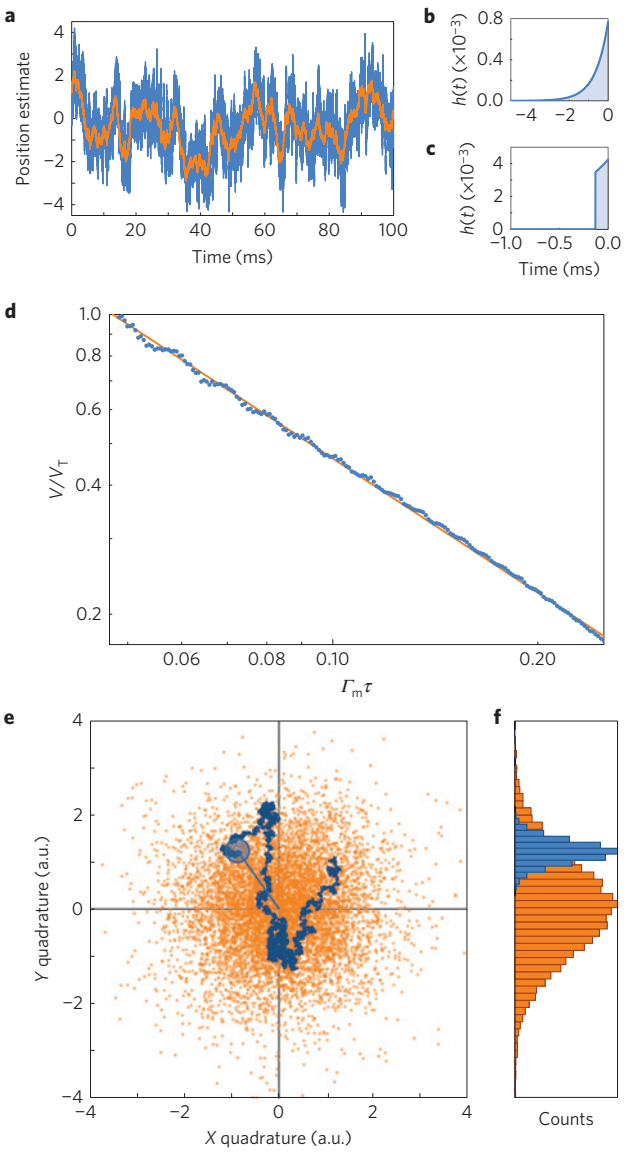

Figure 3 | Real-time measurements of superfluid motion. a, Estimate of the superfluid position in the X quadrature. The X and Y quadratures are given by $X(t) = h(t) * i(t) \cos(\omega_m t)$, $Y(t) = h(t) * i(t) \sin(\omega_m t)$, where $*$ is a convolution and $i(t)$ is the measured photocurrent, which is filtered with an exponentially decaying filter, $h(t) = Ae^{-2\Gamma_m|t|}(H(t+\tau) - H(t))$, where A is chosen so that $\int h(t)dt$ is constant for filters with different measurement times, and $H(t)$ is the Heaviside step function. The orange and blue traces, respectively, represent a best estimate X_{best} obtained by taking $\tau \to \infty$, and the estimate X obtained using $\tau = 1/(10\Gamma_m)$, with the corresponding filters shown in **b** and **c**. Measurements were made on the 482 kHz mode at the base temperature of the cryostat (530 mK). **b**,**c**, Exponentially decaying filters used in the X-quadrature analysis. **d**, The ratio of the measurement variance, $V = \langle (X(t) - X_{best}(t))^2 \rangle$, to the thermal variance, $V_T = \langle X_{best}^2 \rangle$, as the measurement time is varied. **e**, Thermal motion of the superfluid mode in phase space. Each orange point is the position of the oscillator, measured in a time $1/\Gamma_m$. The blue circle represents the uncertainty of an individual measurement, defined as the standard deviation of the shot noise in the measurement time. The dark blue line shows an example trajectory of the oscillator obtained by making successive measurements, tracking its motion in real time over a period of 5 ms. **f**, Histogram of the position of the superfluid (orange) and the measurement noise (blue) shown in **e**. Both the superfluid position and measurement uncertainty are normally distributed. Statistics were built up by binning the result of 8,000 individual measurements taken over 5 s of data acquisition.

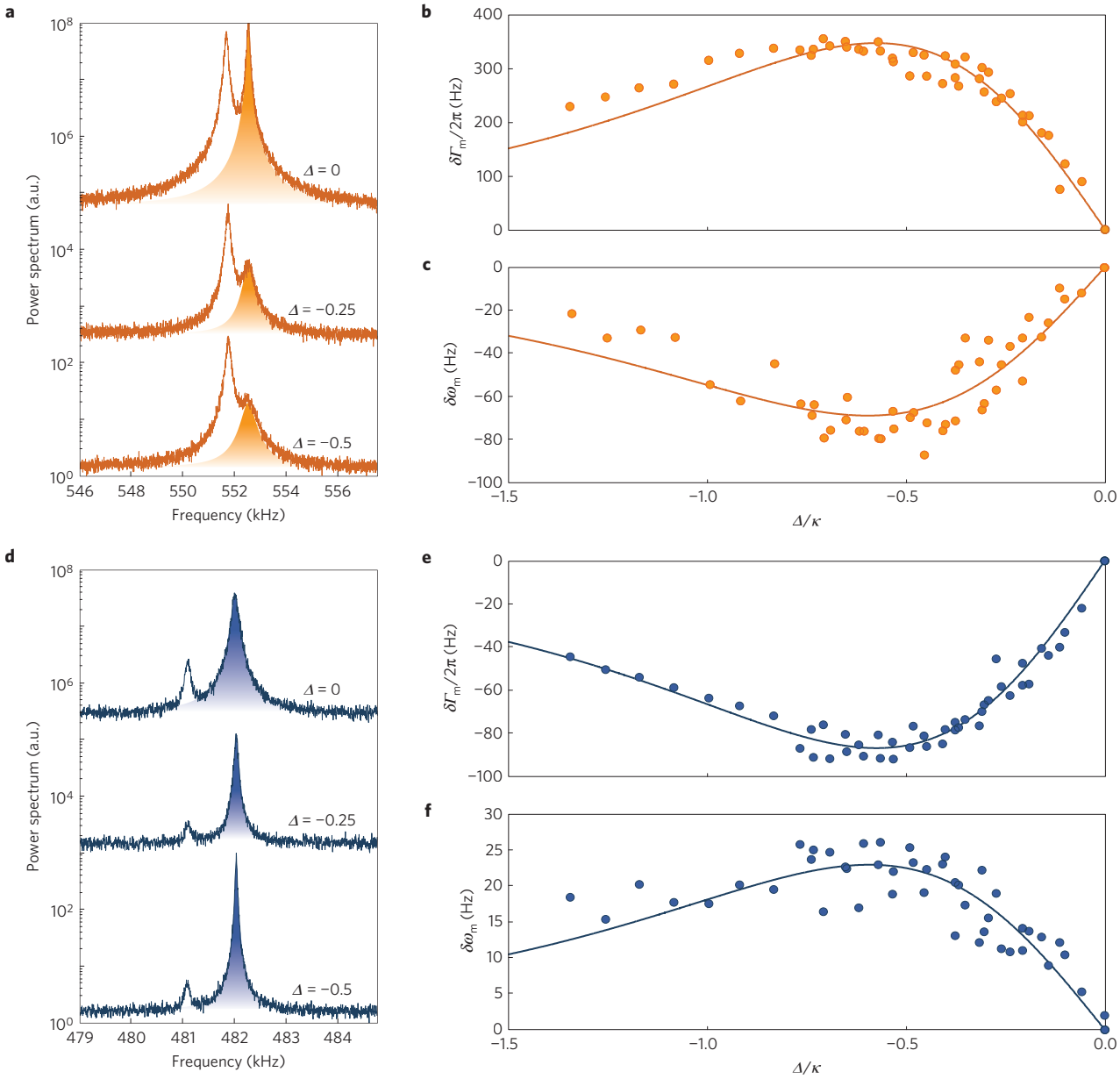

Figure 4 | Optomechanical heating and cooling of two third sound modes. Detuning the optical field results in cooling (**a**) or heating (**d**) of the superfluid excitations. The laser is red-detuned with respect to the cavity for both the 552.5 kHz mode and the 482 kHz mode. Whether the mode experiences heating or cooling depends on the relative magnitude of the radiation pressure force and the sign of the photothermal constant (β), which itself depends on the optical and mechanical mode. **a**, Spectra of two closely spaced mechanical modes around 552.5 kHz with varying optical detuning. The shaded mode experiences photothermally induced broadening ($\beta > 0$), with the mechanical linewidth increasing with increasing red detuning. **b**,**c**, Change in mechanical damping rate and mechanical resonance frequency as a function of detuning for the 552 kHz mode. A maximum relative frequency shift of $\delta\omega_m/2\pi = -60$ Hz is measured at $\Delta = -0.60\kappa$. Solid line: theoretical fit to photothermal broadening. **d**, Spectra of two closely spaced mechanical modes around 482 kHz with varying optical detuning. The shaded mode experiences photothermally induced narrowing ($\beta < 0$), with the mechanical linewidth decreasing with increasing red detuning. **e**,**f**, Change in mechanical damping rate and mechanical resonance frequency as a function of detuning for the 482 kHz mode. A maximum relative frequency shift of $\delta\omega_m/2\pi = 23$ Hz is measured at $\Delta = -0.60\kappa$. Solid line: theoretical fit to photothermal narrowing. Traces in **a** and **d** are offset for clarity. All detuning measurements were taken with 200 nW of launched optical power.

the thermal variance at a measurement time of 121 μs; a factor of 11 times shorter than $1/\Gamma_m$ (1.3 ms), and therefore sufficient to track the superfluid motion in real time (see Supplementary Information VII for a theoretical discussion). Figure 3e shows a thermal trajectory of the superfluid mode, tracked in real time from a sequence of measurements each having 1.3 ms duration. As can be seen from Fig. 3f, it was possible to track the thermal trajectory of the oscillator with precision a factor of 4.0 below the thermomechanical noise.

Thermometry and cooling of superfluid excitations

The ability to resolve the thermal motion of the superfluid allows thermometry to be performed on superfluid modes. Locking the laser to the cavity resonance, it is possible to probe the effect of the optical field on the superfluid modes in the absence of dynamical optomechanical backaction. Spectral analysis of the modes in this regime reveals an increase in mode temperature and linewidth with laser power. Thermometry of a microtoroid mechanical mode shows that this is not due to bulk optical heating

(see Supplementary Information V). This is further evidenced by the scaling of both temperature and linewidth with optical power, which was observed to be sub-linear. Nonlinear scaling of this form has been observed in other optomechanical systems[32], and can be explained by the presence of an independent bath, coupled to the superfluid mode, and driven out of equilibrium by the optical field (see Supplementary Information V).

Dynamical backaction due to both radiation pressure and photothermal forces, such as photoconvective actuation[31], provides a mechanism to cool or heat mechanical excitations. To experimentally probe these effects we red-detune the optical field from the cavity resonance and observe modifications to the mechanical resonance frequency and dissipation rate (Fig. 4). It was found that the dynamical backaction is dominated by photothermal forces[33] and varied significantly between third sound modes. This variation can be attributed to differences in the overlap of the modes with the photoconvective flow field generated by optical heating (see Supplementary Information VI). Most strikingly, for near-degenerate pairs of modes, the dynamical backaction was consistently considerably stronger on the higher-frequency mode (see, for example, Fig. 4a,d). Although with current experiments it is not possible to reach a definitive conclusion as to the cause of this effect, we expect that it is due to the defect on the microtoroid surface shown in Fig. 1b (inset). This defect breaks the cylindrical symmetry not only of the third sound modes, but also of the photoconvective flow field. Third sound modes with symmetry matching the flow field will be effectively driven, whereas the driving of those that are anti-symmetric will be greatly suppressed.

The overlap between superfluid flow and third sound modes determines not only the strength, but also the sign, of the photothermal response, as illustrated here for third sound modes at 552.5 and 482 kHz (Fig. 4). The 552.5 kHz mode shows linewidth broadening from $\Gamma_0/2\pi = 115$ Hz on-resonance to $\Gamma_\Delta/2\pi = 464$ Hz at a detuning of $\Delta = -0.58\kappa$, as well as spring softening (Fig. 4b,c). The 482 kHz mode, by contrast, shows linewidth narrowing and spring stiffening with increasing red detuning (Fig. 4d), indicating that here the photothermal coefficient is negative, opposing the direction of radiation pressure. At a detuning of $\Delta = -0.58\kappa$ the linewidth has narrowed to $\Gamma_\Delta/2\pi = 49$ Hz from $\Gamma_0/2\pi = 137$ Hz on-resonance. In both cases, the behaviour agrees well with photothermal theory (see Supplementary Information VI), as seen by the fit in Fig. 4b,c,e,f. Mode-dependent photothermal responses of this kind have been previously reported in the context of a fibre-cavity-coupled AFM microcantilever[34], where optically induced heating at the tip of the cantilever causes opposing photothermal responses between the first- and second-order mechanical modes. From the change in damping rate we find that, in our case, detuning cools the 552.5 kHz third sound mode by a maximum factor of $T_\Delta/T_0 = \Gamma_0/\Gamma_\Delta = 0.25$, and heats the 482 kHz third sound mode by as much as $T_\Delta/T_0 = 2.8$. Although the level of cooling observed here is relatively modest, we note that photothermal cooling is not fundamentally limited and can, in principle, approach the quantum ground state[33].

Compared to other cavity optomechanics experiments that use photothermal coupling, the photothermal effect observed here is exceptionally fast owing to the high thermal conductivity of superfluid helium[5]. The characteristic time constant τ_t can be deduced from the functional form of the photothermal response seen in Fig. 4b,c,e,f, and is found to be $\tau \approx 600$ ns.

Concluding remarks

Observations of the thermally driven trajectories of vortex cores in bulk superfluid helium provide insight into vortex–vortex interactions and the dissipation of sound via vortex–phonon interactions (see for example ref. 8). Our paper reports the complementary capabilities to both track and control the thermodynamic motion of phonon excitations. This provides a new tool to study the dynamics and interactions of elementary excitations in superfluid helium. Our work opens the door to study the thermally driven behaviour of superfluid phonon excitations both in, and outside of, equilibrium, and thereby extend recent efforts to test the microscopic validity of fluctuation theorems and fundamental aspects of statistical mechanics into superfluid systems[35].

In general, interactions are enhanced as systems become increasingly confined. In superfluid helium, for instance, the single phonon–vortex interaction rate scales as the inverse square of the confining length scale. In our devices, this rate is approximately 10 Hz, four orders of magnitude larger than any previous experiment[2], and only a factor of ten smaller than the phonon dissipation rate. As a consequence, our devices offer the prospect to resolve vortex–phonon dynamics in real time with as few as ten unpaired vortices, combined with an atomically smooth surface finish that reduces the occurrence of pinned vortices. Although there remains significant debate about the dominant dissipation mechanisms in two-dimensional superfluid helium, phonon–vortex interactions are thought to play a crucial role[1]. Phonon–vortex interactions are also important for as-yet untested predictions such as the formation of Onsager vortices as two-dimensional superfluids evolve[36] and the decay of two-dimensional superfluid turbulence at zero temperature[37,38], as well as for Berezinskii–Kosterlitz–Thouless (BKT) physics near the phase transition[39].

With a factor of three reduction in diameter, it should be possible to reach the strong coupling regime in our devices, where the single phonon–vortex interaction rate is larger than both phonon and vortex dissipation rates. This offers the prospect of studying a new, previously unexplored regime of BKT physics. Such physics would be further augmented by the capacity to laser control and cool individual phonon modes demonstrated here. Although laser cooling is routinely achieved in solid- and gas-phase systems such as cold atom physics, ion trapping, atomic clocks and optomechanics, it has not previously been demonstrated in superfluid helium, or indeed in any liquid.

We finally observe that superfluid films may open new regimes of cavity optomechanics. Hybridized phonon–vortex modes may allow experiments where the optical field is strongly coupled to the motion of vortices. Furthermore, third sound modes have been observed in helium films thinner than a single atomic layer[27]. This regime is inherently highly nonlinear, with mechanical zero-point fluctuations large compared to the film thickness. In sensing applications, atom interferometry with superfluid helium enables precise force and inertial sensing. The ability to resolve the thermomechanical motion of the fluid demonstrated here could enable superfluid force and inertial sensors that operate at the thermal noise limit, a capability which until now has not been possible.

Received 15 June 2015; accepted 3 March 2016;
published online 4 April 2016

References

1. Hoffmann, J. A., Penanen, K., Davis, J. C. & Packard, R. E. Measurements of attenuation of third sound: evidence of trapped vorticity in thick films of superfluid He-4. *J. Low Temp. Phys.* **135,** 177–202 (2004).
2. Ellis, F. M. & Luo, H. Observation of the persistent-current splitting of a 3rd-sound resonator. *Phys. Rev. B* **39,** 2703–2706 (1989).
3. Barenghi, C. F., Skrbek, L. & Sreenivasan, K. R. Introduction to quantum turbulence. *Proc. Natl Acad. Sci. USA* **111,** 4647–4652 (2014).
4. Bishop, D. J. & Reppy, J. D. Study of the superfluid transition in two-dimensional films. *Phys. Rev. Lett.* **40,** 1727–1730 (1978).
5. Tilley, D. & Tilley, J. *Superfluidity and Superconductivity* (CRC, 1990).

6. Bramwell, S. T. & Keimer, B. Neutron scattering from quantum condensed matter. *Nature Mater.* **13,** 763–767 (2014).
7. Pike, E. R., Vaughan, J. M. & Vinen, W. F. Brillouin scattering from superfluid He-4. *J. Phys. C* **3,** L40 (1970).
8. Fonda, E., Meichle, D. P., Ouellette, N. T., Hormoz, S. & Lathrop, D. P. Direct observation of Kelvin waves excited by quantized vortex reconnection. *Proc. Natl Acad. Sci. USA* **111,** 4707–4710 (2014).
9. Brooks, J. S., Ellis, F. M. & Hallock, R. B. Direct observation of third-sound mass displacement waves in unsaturated superfluid films. *Phys. Rev. Lett.* **40,** 240–243 (1978).
10. De Lorenzo, L. A. & Schwab, K. C. Superfluid optomechanics: coupling of a superfluid to a superconducting condensate. *New J. Phys.* **16,** 113020 (2014).
11. Aspelmeyer, M., Kippenberg, T. J. & Marquardt, F. Cavity optomechanics. *Rev. Mod. Phys.* **86,** 1391–1452 (2014).
12. Bowen, W. P. & Milburn, G. *Quantum Optomechanics* (CRC, 2016).
13. Palomaki, T. A., Teufel, J. D., Simmonds, R. W. & Lehnert, K. W. Entangling mechanical motion with microwave fields. *Science* **342,** 710–713 (2013).
14. Brooks, D. W. C. *et al*. Non-classical light generated by quantum-noise-driven cavity optomechanics. *Nature* **488,** 476–480 (2012).
15. Verhagen, E., Deleglise, S., Weis, S., Schliesser, A. & Kippenberg, T. J. Quantum-coherent coupling of a mechanical oscillator to an optical cavity mode. *Nature* **482,** 63–67 (2012).
16. Riedinger, R. *et al*. Non-classical correlations between single photons and phonons from a mechanical oscillator. *Nature* **530,** 313–316 (2016).
17. Wollman, E. E. *et al*. Quantum squeezing of motion in a mechanical resonator. *Science* **349,** 952–955 (2015).
18. Pirkkalainen, J.-M., Damskägg, E., Brandt, M., Massel, F. & Sillanpää, M. Squeezing of quantum noise of motion in a micromechanical resonator. *Phys. Rev. Lett.* **115,** 243601 (2015).
19. Lecocq, F., Clark, J., Simmonds, R., Aumentado, J. & Teufel, J. Quantum nondemolition measurement of a nonclassical state of a massive object. *Phys. Rev. X* **5,** 041037 (2015).
20. Metcalfe, M. Applications of cavity optomechanics. *Appl. Phys. Rev.* **1,** 031105 (2014).
21. Krause, A. G., Winger, M., Blasius, T. D., Lin, Q. & Painter, O. A high-resolution microchip optomechanical accelerometer. *Nature Photon.* **6,** 768–772 (2012).
22. Forstner, S. *et al*. Ultrasensitive optomechanical magnetometry. *Adv. Mater.* **26,** 6348–6353 (2014).
23. Agarwal, G. S. & Jha, S. S. Theory of optomechanical interactions in superfluid He. *Phys. Rev. A* **90,** 023812 (2014).
24. Penanen, K. & Packard, R. E. A model for third sound attenuation in thick He-4 films. *J. Low Temp. Phys.* **128,** 25–35 (2002).
25. Armani, D. K., Kippenberg, T. J., Spillane, S. M. & Vahala, K. J. Ultra-high-Q toroid microcavity on a chip. *Nature* **421,** 925–928 (2003).
26. Atkins, K. R. Third and fourth sound in liquid helium ii. *Phys. Rev.* **113,** 962–965 (1959).
27. Shirron, P. J. & Mochel, J. M. Atomically thin superfluid-helium films on solid hydrogen. *Phys. Rev. Lett.* **67,** 1118–1121 (1991).
28. Anetsberger, G. *et al*. Near-field cavity optomechanics with nanomechanical oscillators. *Nature Phys.* **5,** 909–914 (2009).
29. Harris, G. I., Andersen, U. L., Knittel, J. & Bowen, W. P. Feedback-enhanced sensitivity in optomechanics: surpassing the parametric instability barrier. *Phys. Rev. A* **85,** 061802 (2012).
30. Riviere, R., Arcizet, O., Schliesser, A. & Kippenberg, T. J. Evanescent straight tapered-fiber coupling of ultra-high Q optomechanical micro-resonators in a low-vibration helium-4 exchange-gas cryostat. *Rev. Sci. Instrum.* **84,** 043108 (2013).
31. McAuslan, D. L. *et al*. Microphotonic forces from superfluid flow. Preprint at http://arxiv.org/abs/1512.07704 (2015).
32. Meenehan, S. M. *et al*. Silicon optomechanical crystal resonator at millikelvin temperatures. *Phys. Rev. A* **90,** 011803 (2014).
33. Restrepo, J., Gabelli, J., Ciuti, C. & Favero, I. Classical and quantum theory of photothermal cavity cooling of a mechanical oscillator. *C. R. Phys.* **12,** 860–870 (2011).
34. Jourdan, G., Comin, F. & Chevrier, J. Mechanical mode dependence of bolometric backaction in an atomic force microscopy microlever. *Phys. Rev. Lett.* **101,** 133904 (2008).
35. Bustamante, C., Liphardt, J. & Ritort, F. The nonequilibrium thermodynamics of small systems. *Phys. Today* **58,** 43–48 (July, 2005).
36. Simula, T., Davis, M. J. & Helmerson, K. Emergence of order from turbulence in an isolated planar superfluid. *Phys. Rev. Lett.* **113,** 165302 (2014).
37. Kozik, E. & Svistunov, B. Vortex-phonon interaction. *Phys. Rev. B* **72,** 172505 (2005).
38. Davis, S. I., Hendry, P. C. & McClintock, P. V. E. Decay of quantized vorticity in superfluid 4He at mK temperatures. *Physica B* **280,** 43–44 (2000).
39. Kosterlitz, J. M. & Thouless, D. J. Ordering, metastability and phase transitions in two-dimensional systems. *J. Phys. C* **6,** 1181–1203 (1973).

Acknowledgements

This research was funded by the Australian Centre for Engineered Quantum Systems (CE110001013). Micro-fabrication was performed at the Queensland Node of the Australian National Fabrication Facility (ANFF-Q). W.P.B. was supported by the ARC Future Fellowship FT140100650. The authors thank G. A. Brawley, M. J. Davis, B. J. Powell and Z. Duan for valuable discussions.

Author contributions

G.I.H. and D.L.M. conducted the experiments and contributed equally to this work. G.I.H., D.L.M. and W.P.B. formulated the theory, analysed the data and wrote the manuscript. Micro-fabrication was performed by D.L.M. and E.S., and C.B. and Y.S. contributed to the experiments. The project was led by W.P.B.

Additional information

Supplementary information is available in the online version of the paper. Reprints and permissions information is available online at www.nature.com/reprints. Correspondence and requests for materials should be addressed to W.P.B.

Competing financial interests

The authors declare no competing financial interests.